Non-uniformly Spaced Antenna Arrays with Overlapped Elements Constraint

Noor Mohammed Qassim and Jafar Ramadhan Mohammed

Ninevah University, Mosul, Iraq

https://doi.org/10.26636/jtit.2024.4.1740

Abstract — In the literature, inter-element spacing antenna design methods have been widely discussed and presented as an alternative approach to element excitation amplitude and/or phase control methods that may be relied upon to achieve the required array pattern shapes. However, methods associated with non-uniformly distributed elements suffer from the element overlap problem, where some of the optimized element locations may overlap each other and cause changes in the overall array aperture length. Practically, these element overlaps cannot be implemented, due to the physical antenna element size, without omitting some of them. Consequently, the overall performance of the antenna array is degraded. Further, degradation may occur when considering phased arrays with scanned main beams. In this paper, we first illustrate the effect of the problem of overlapped element locations and then we propose two approaches based on the genetic algorithm to optimize non-uniformly spaced arrays with overlapped element locations, while simultaneously preserving the array's directivity. To solve the problem of overlapping and to determine the physical array element size, the minimum element-spacing constraints are incorporated in a simple way in the proposed approaches. Thus, the time required to perform optimization-related computations is greatly reduced. Simulation results confirm the effectiveness of the two proposed solutions, where the probability of the elements overlapping has been reduced to zero under specific conditions related to the locations of the some of the elements, while the peak sidelobe levels were always kept below –15 dB and directivity was maintained, to the extent possible, at the level of that of standard uniformly spaced arrays.

Keywords — element location overlaps, non-uniformly spaced arrays, phased antenna arrays, sidelobe level minimization

1. Introduction

In the process of synthesizing an antenna array, several design variables which can be efficiently controlled to achieve the desired beam pattern shapes offering low sidelobe level, limited beam width and good directivity need to be taken into consideration. These include the separation distances between the array's elements (or absolute element locations), amplitude weighting and/or phase weighting of the array element excitation vector. The amplitude and/or phase weighting-based design methods with uniformly spaced elements (i.e. fixed element locations) are referred to as electronic approaches, with the array patterns being reshaped electronically, and the element locations remaining fixed and uniform. The unequally spaced array methods are referred to as mechanical approaches, as the array patterns are mechanically reshaped by changing the locations of the specific elements. In the case of automated scanning beam arrays, both mechanical and electronic approaches require controllable phase shifters to achieve wide-angle beam scanning. These phase shifters are separate and independent from those used for element excitation phase weighting control [1].

From the point of view of implementing the designs, the feeding network of the electronic approaches requires fine adjustment of the attenuators/amplifiers used for amplitude excitation weighting. Additionally, accurate phase shifters are required for phase excitation weighting of the array's elements, to reshape the array's pattern in accordance with the requirements [2]. Any errors or deviations from those fine values will cause significant and unavoidable changes in the radiation pattern [3], [4]. Therefore, these electronic approaches are very sensitive, relatively costly and require that advanced RF components be used.

On the other hand, mechanical approaches with uniform amplitude excitation weighting have been widely used due to the need for a simple feeding divider network which can be implemented without any attenuators or amplifiers. Therefore, no sensitivity-related errors can be made [5]. These advantages have recently motivated many researchers from around the world to fully explore the benefits of these types of arrays [6]–[10].

Further, non-uniformly spaced arrays are expected to be more popular in current and future wireless communication systems due to their great array pattern reshaping capability. In order to meet some desirable requirements, several user-defined constraints may be introduced concerning either the array's geometry itself (the number of elements and the spacing between them) its radiation pattern (minimum sidelobe level and limited beamwidth). These constraints mean that the synthesis of such arrays becomes a non-linear problem [11] requiring efficient optimization techniques. Thus, various evolution algorithms, such as the genetic algorithm (GA) [12], [13], differential evolution (DE) [14], particle swarm optimization (PSO) [15] and the whale optimization algorithm (WOA) [16] have been used to solve this non-linear problem.

Other solutions determine an optimal combination of feeding current and inter-element spacing to produce array patterns with the lowest sidelobe level, improved beamwidth, and maximum directivity [17]. Moreover, the thinning process produces non-uniform inter-element spacing and it has been exploited to minimize sidelobe levels [18], [19]. However, thinned arrays need a very high number of combinations to examine all potential element locations. Thus, non-uniformly spaced arrays obtained with the use of the thinning process are very time consuming to produce [20]. Therefore, determination of inter-element spacing or element locations may provide greater control over the shape of the array's radiation pattern than thinning methods.

Recently, a T-shaped clustered array [21], a circular boundary array [22] and control over the position of selected elements [23] have been also relied upon for sidelobe reduction. Other methods use a redundancy elimination technique to synthesize large-scale planar isophoric sparse arrays in order to achieve low sidelobe levels. In this approach, the theoretical limits for the achievable minimum spacing and aperture are calculated to enable selective retention of non-redundant positional constraints only [24]. In [25], an alternating convex optimization was suggested to synthesize non-uniformly spaced arrays with minimum element spacing constraints.

In this paper, the problem of element location overlap, which is unavoidable when optimizing the absolute element locations using all non-uniformly spaced methods, is addressed. Then, two efficient solutions based on the bounding location limits are suggested to prevent this problem from occurring. Finally, a comprehensive and optimized method for designing non-uniformly spaced arrays with minimum element spacing constraints and improved response time is presented. This problem becomes more significant and may include all or most of the array element locations when imposing more user-defined constraints and steering the main beams towards direction other than the normal referenced direction. Thus, the process of designing such arrays in practice calls for increased attention.

Finally, it is worth mentioning that the problem of overlapping element locations in non-uniformly spaced arrays has not been fully discussed and addressed in the literature and continues remains a truly challenging issue that needs to be resolved.

2. Principles of the Proposed Method

2.1. Formulation of the Element Overlap Problem

Non-uniform spacing between the array's elements may be expressed in terms of inter-element spacing d_n or actual element location with respect to the center of the array x_n. The overall array pattern AP, which is a product of element pattern EP and array factor AF (being equal to inter-element spacing d_n) for N even and symmetrical radiating elements can be written as:

$$\begin{aligned} AP(u) &= EP(u) \times AF(u) \\ &= \sum_{n=1}^{\frac{N}{2}} a_n \cos\left[(n-0.5)k\, d_n(u-u_o)\right], \end{aligned} \tag{1}$$

where $u = \sin(\theta)$, θ is the elevation angle within the range of $0 \leqslant \theta \leqslant \pi$, $EP(u)$ is the element pattern which is equal to one for isotropic radiators, a_n is the complex (amplitude and phase) weighting of the n-th element in the array which is equal to $a_n = 1$ for unit-amplitude weighting, $k = \frac{2\pi}{\lambda}$, and u_o is the steering direction of the main beam.

Equation (1) can be rewritten – in terms of element locations x_n as follows:

$$AP(u) = \sum_{n=1}^{\frac{N}{2}} a_n \cos\left[k\, x_n(u-u_o)\right]. \tag{2}$$

To clearly explain the difference between Eqs. (1) and (2), it is important to determine the bounds concerning both minimum and maximum potential values of both d_n and x_n, as they need to be examined by the optimizer for inter-element spacing $d_n = \Delta(\frac{d}{\lambda})$, $0 \leqslant \Delta \leqslant 1$ and for x_n being $0 \leqslant x_n \leqslant L_{AA}$, where L_{AA} is the length of the array's aperture.

To minimize the peak sidelobe level in the region $FNBW \leqslant |u-u_o| \leqslant 1$ of the array pattern in Eq. (1) or Eq. (2), the following cost function can be used [12]:

$$\text{Cost} = 20\log_{10}\min\big(|AP(u-u_o)|\big), \tag{3}$$

where $FNBW$ is the first null beam width in the array pattern which defines the starting point of the sidelobe region.

Such a cost function minimizes the sidelobes by optimizing either the array element locations x_n or inter-element spacings d_n, according to Eqs. (1) and (2). In both cases, only these two sets of variables, i.e. d_n and x_n, are the design-related parameters that need to be optimized.

In order to keep the beam width and, consequently, the directivity of the optimized non-uniformly spaced array as close as possible to that of the standard uniformly spaced array, the overall array apertures of both of them should be kept the same. Thus, the following location bounds are imposed on the proposed non-uniformly spaced array:

$$\begin{gathered} \frac{d}{2} \leqslant x_n \leqslant L_{UAA} \text{ with } L_{UAA} = x\left(\frac{N}{2}\right), \\ n = 1, 2, \ldots, \frac{N}{2}, \end{gathered} \tag{4}$$

where L_{UAA} is the aperture length of the standard uniformly spaced array.

From this equation, it can be seen that the locations of the first and last elements on the right side of the array center were fixed at $x_1 = \frac{d}{2}$ and $x_{\frac{N}{2}} = L_{UAA}$. Locations of other elements in between can be optimized according to the cost function given in Eq. (3).

The locations of the in-between elements are random. Thus, there is a great chance that an element may be placed over another element or that they may located close to each other. Therefore, physical element size overlaps are unavoidable in these types of arrays.

To illustrate this problem, let us consider an array of $N = 40$ elements that are distributed symmetrically around the array's center. By fixing the location of the first element on each side of the array only, $\frac{N}{2} - 1$ element locations can be optimized according to Eq. (3). The number of controlled element locations is 19 on each side of the array, while the first element was fixed at the original uniformly spaced elements $x_1 = \frac{d}{2}$.

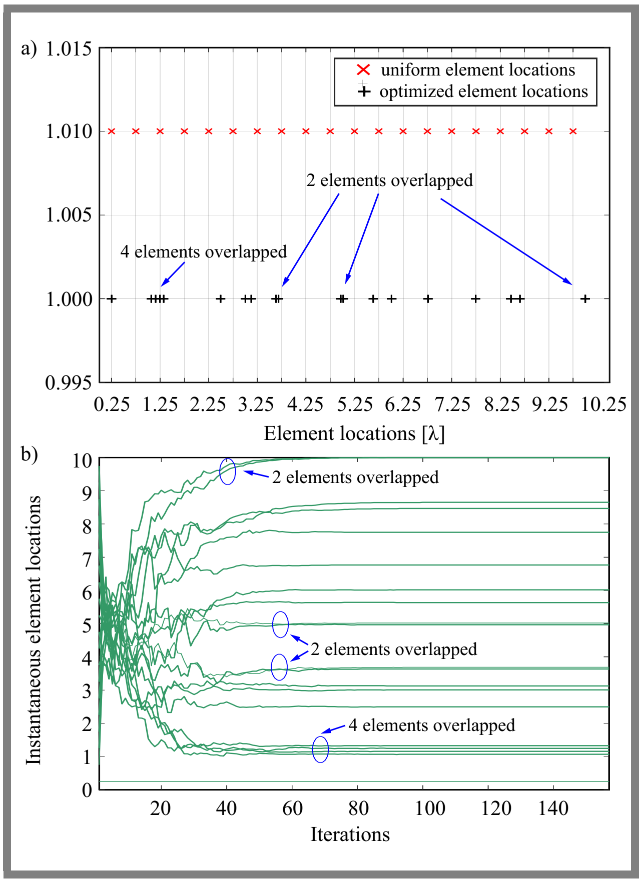

Fig. 1. Array element overlaps: a) element locations and b) instantaneous element locations.

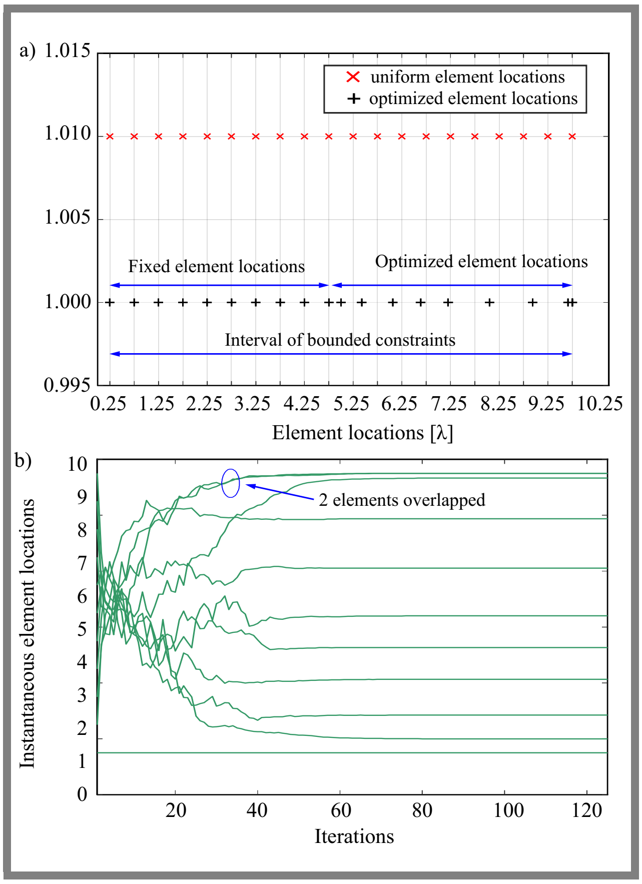

Fig. 2. Partially controlled element location approach: a) element locations and b) instantaneous element locations.

Further, we assumed that the steered direction of the main beam is $u_o = 0.6$ radians in u-space. Figure 1 shows the resultant element locations of the optimized array. The standard array geometry that uses uniformly spaced elements has been also shown for comparison. One may notice that the most of the resultant optimized element locations overlap. Therefore, such a design configuration without overlapped elements is practically impossible.

2.2. Proposed Solutions

In this section, we present two approaches to dealing with the problem of element location overlaps.

The first approach is based on controlling the locations of a number of outer elements instead of all element locations, as shown in Fig. 2. The locations of inner elements remain fixed and match the locations of the original uniformly spaced array elements. By optimizing the locations of outer elements only, we will reduce the probability of overlapping and will mitigate the array's implementation cost. The probability of overlapping is reduced, but the phenomenon cannot be prevented entirely.

This approach also offers a level of directivity that is higher than the one achieved when relying on fully optimized element locations. The only loss is a slight increase in the sidelobe level, when compared to that of the fully optimized element locations. This is mainly due to the lower number of degrees of freedom available.

The second approach is based on enforcing constraints on the location of each element, as shown in Fig. 3. This allows to completely prevent the overlapping of specific elements while simultaneously preserving the array's performance without sacrificing sidelobe level, due to the availability of all degrees of freedom. The applied bound constraints can be written as follows:

$$x_{uniform_n} - \Delta \leqslant x_n \leqslant x_{uniform_n} + \Delta, \;\; n = 1, 2, \ldots, \frac{N}{2}, \quad (5)$$

where $x_{uniform_n}$ is the location of the n-th element of the standard uniformly spaced array and Δ is the bound constraint for lower and upper intervals which can be specified by the user.

The design steps may be summarized as follows:

1) Define the initial parameters, such as array parameters, population size, and the variable number of element locations.
2) Set the goals or user-defined constraints related to array element locations that can be provided by the designer.
3) Set the optimization parameters, such as parents, mutation, crossover, and the maximum number of iterations. Calculate and sort the cost function values.
4) Perform genetic optimization which includes mirage process, choosing best siblings and mutations.
5) Perform best pattern calculation.

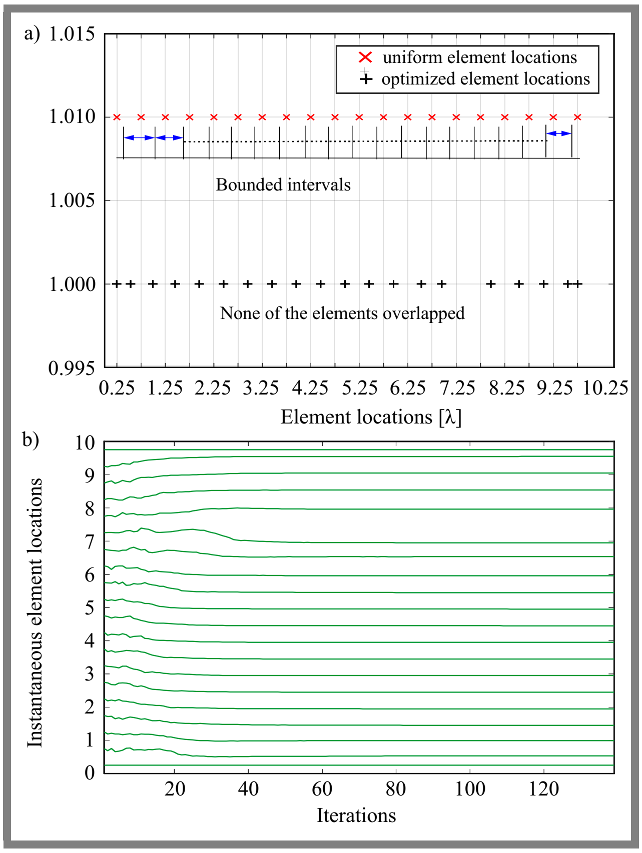

Fig. 3. The bound constraints approach: a) element locations and b) instantaneous element locations.

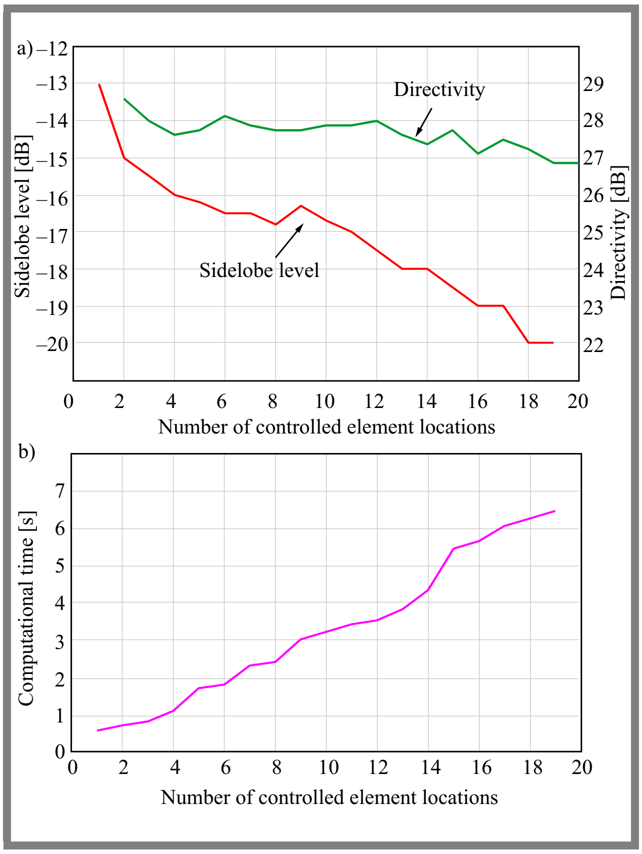

Fig. 4. SLL variation versus number of controlled element locations and directivity variation for unscanned main beam $u_o = 0°$ a) and computational time b).

3. Simulation Results

In all of the considered scenarios, a symmetric phased array of $N = 40$ radiating elements with either fully or partially non-uniformly spaced elements was examined. For the genetic optimization algorithm used, the size of the population is set to 100. The remaining parameters were chosen in the following manner: uniform crossover, selection was tournament, and the mutation rate was 0.2. Finally, the mating pool was chosen to be 4. The main beam has been steered to remain within the range of the elevation plane between $-0.5 \leqslant u_o \leqslant 0.5$.

In the first example, performance in terms of sidelobe level (SLL), directivity (D), and the computational time of the proposed non-uniformly spaced array was studied for various controlling element locations. Figure 4 illustrates SLL and D variations, as well as the required computational time.

Generally, one may notice from these two figures that SLL reduction improves as the number of controlled element locations increases, while the D parameter is slightly degraded and the computational time becomes longer when increasing the number of the controlled element locations.

In the second example, SLL variations with the scan angle of the main beam are illustrated in Fig. 5. Here, three instances of non-uniformly spaced arrays were considered and compared. In the first instance, full control is exercised over all element locations (i.e. all element locations are optimized), while in the second and third instances, half or quarter of element locations are controller, respectively. The main beam has

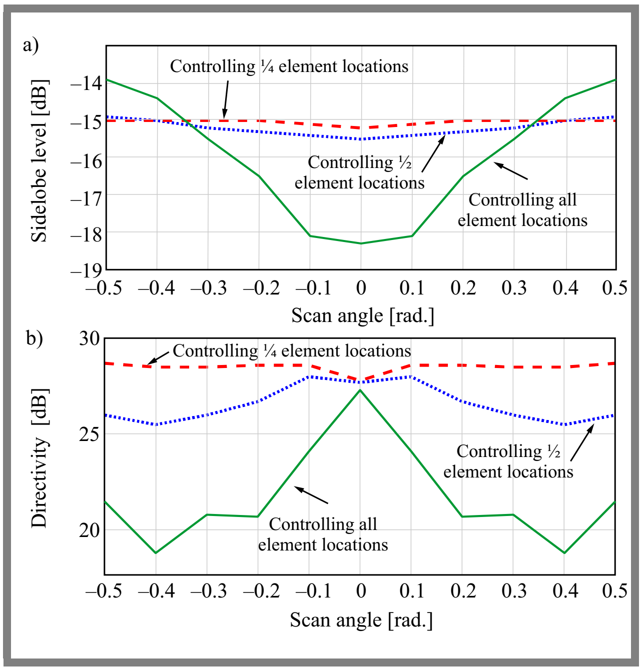

Fig. 5. SLL variation versus scan angle a) and directivity variation for three element location control instances b).

been steered in a range of $-0.5 \leqslant u_o \leqslant 0.5$ in the u-space. Directivity was evaluated using the same procedure.

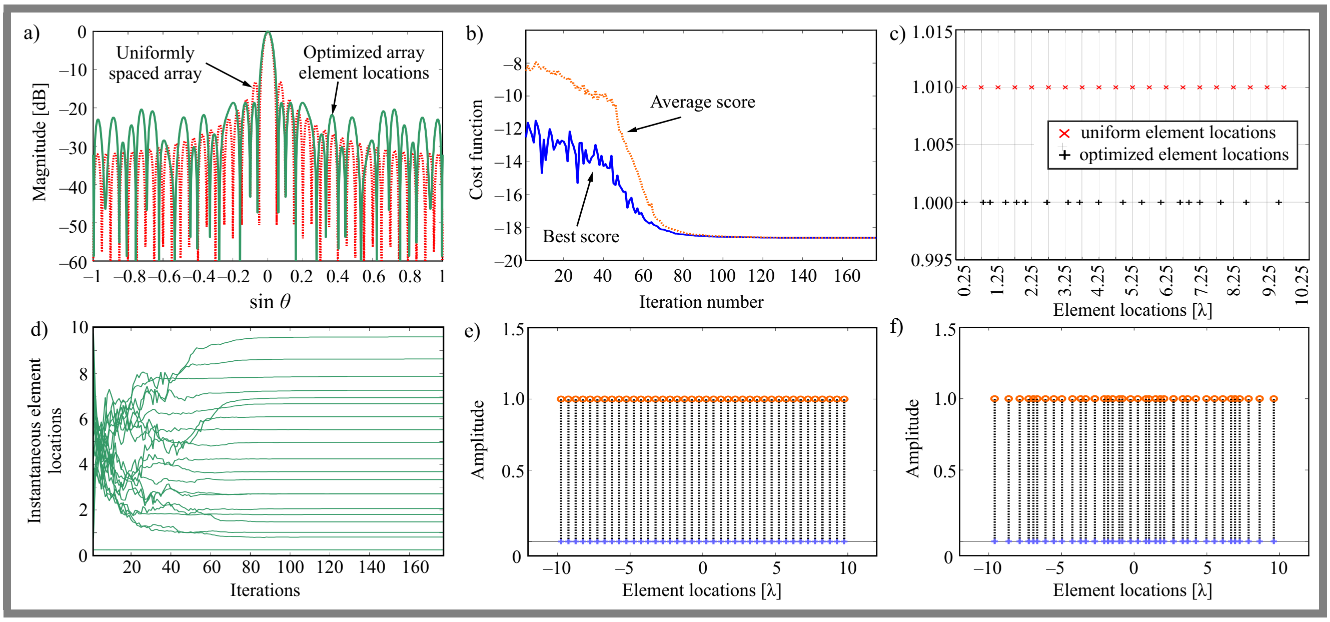

Fig. 6. Results of controlling all element locations: a) radiation patterns, b) cost function variations, c) element locations, d) their instantaneous variations, and e–f) element amplitude weights.

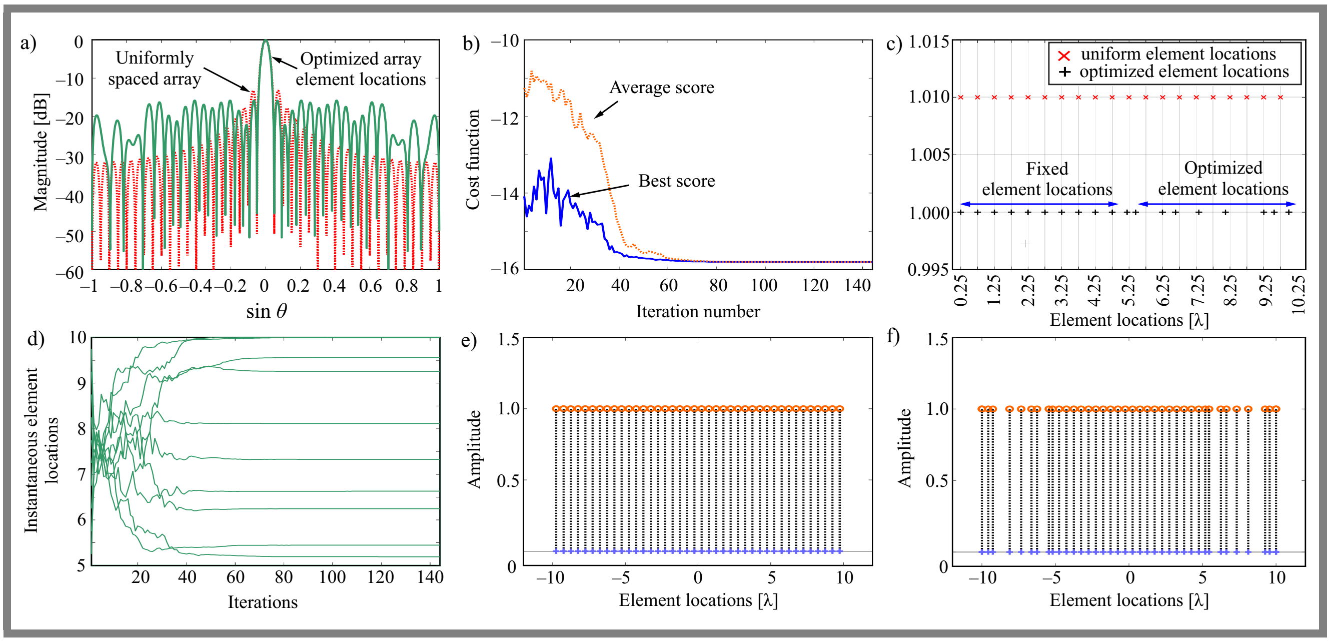

Fig. 7. Results of controlling half element locations: a) radiation patterns, b) cost function variations, c) element locations, d) their instantaneous variations, and e–f) element amplitude weights.

Further, the results of these three instances in which all, half, and a quarter of the element locations are controlled are shown in Figs. 6–8, respectively.

Directivity D, SLL, and computational time T of these three instances were $D = 27.2$ dB, $SLL = -18.6$ dB, $T = 7.875$ s, $D = 27.3$ dB, $SLL = -15.5$ dB, $T = 5.471$ s, $D = 28.0$ dB, $SLL = -15.2$ dB, $T = 2.27$ s, respectively. The optimized element locations for these three instances were:

- x_{fully}={0.2500 0.8084 1.0179 1.4764 1.8005 2.0588 2.7005 2.7088 3.3348 3.6790 4.2418 4.9666 5.5234 6.0957 6.6634 6.9290 7.2540 7.8689 8.6270 9.5963},
- x_{half}={0.2500 0.7500 1.2500 1.7500 2.2500 2.7500 3.2500 3.7500 4.2500 4.7500 5.0000 5.4614 5.9897 6.5948 7.2056 7.9667 8.9249 9.75 9.750 9.75},
- $x_{quarter}$={0.25 0.75 1.25 1.75 2.25 2.75 3.25 3.75 4.25 4.75 5.25 5.75 6.25 6.75 7.25 8.27 9.129 9.75 9.75 9.75}.

One may see that the performance of a partially controlled element locations approach is better in terms of directivity and computational time than that of the fully controlled element locations approach, except for the peak side lobe level which is slightly higher due to a smaller number of degrees of freedom, as mentioned earlier.

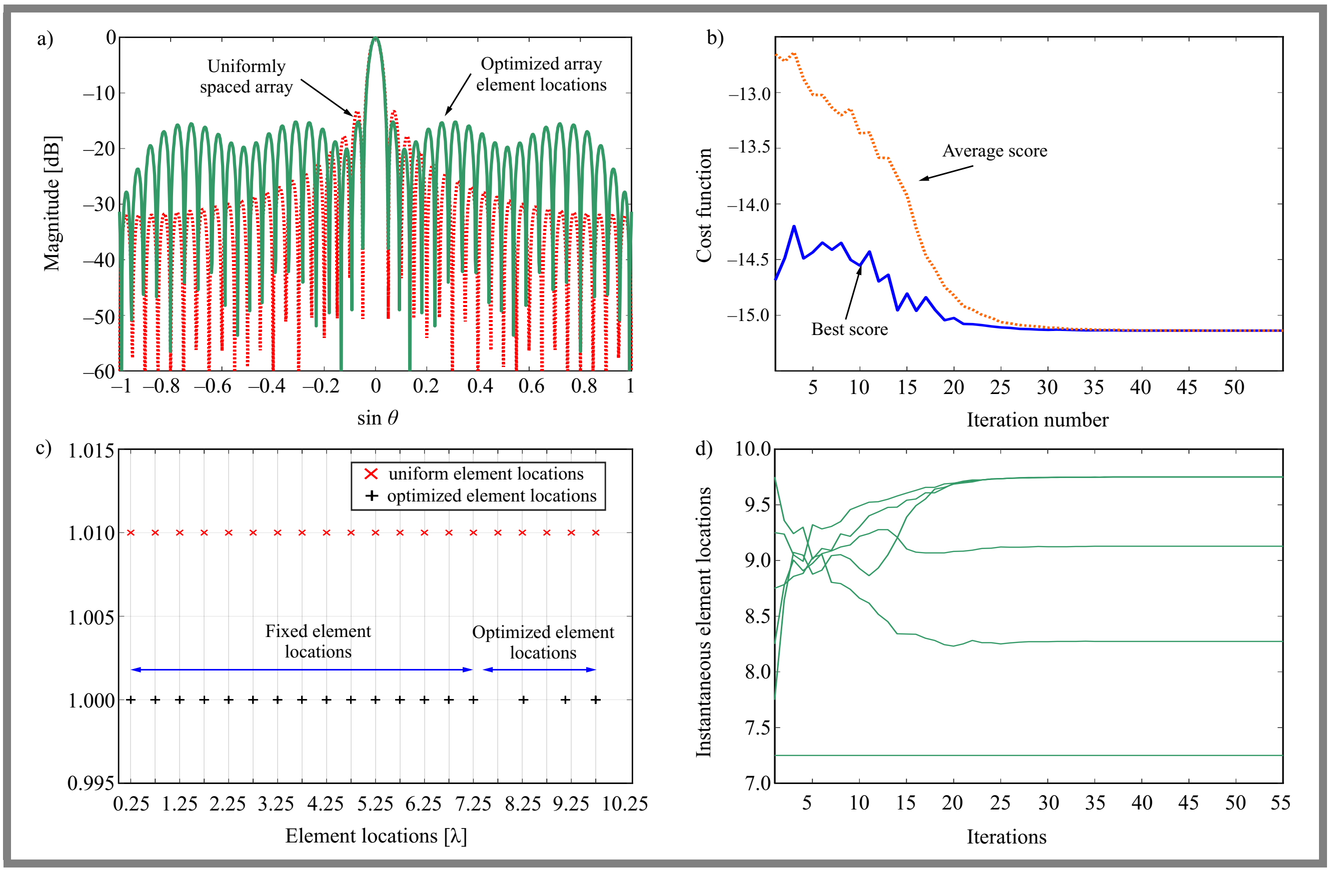

Fig. 8. Results of controlling quarter element locations: a) radiation patterns, b) cost function variations, c) element locations, and d) their instantaneous variations.

More importantly, it can be observed that the element location overlaps still exist, even with the partially controlled element locations approach. This is mainly due to the wide bound constraints used, as shown in Eq. (4), which only preserve the overall array aperture (i.e. beamwidth), with overlaps between optimized element locations not being included.

In the next example, the lower and upper bounded constraints on each controlled element location are considered to prevent overlaps between the array's elements. At first, the proposed approach is applied to the fully controlled element locations method (see Fig. 9), and then to the partially controlled element locations method (see Fig. 10) to assess their performance.

The performance of the fully controlled element locations method with bounded constraints was $D = 27.74$ dB, $SLL = -17.0$ dB, $T = 9.2$ s, and x_n={0.25 0.583 0.9768 1.458 1.952 2.45 2.95 3.45 3.95 4.45 4.95 5.45 5.9679 6.4929 6.95 7.9717 8.5386 9.0496 9.55 9.75}.

For the partially controlled element locations method with bounded constraint, the achieved parameters were: $D = 27.66$ dB, $SLL = -16$ dB, $T = 5.1$ s, and x_n={0.25 0.496 1.25 1.45 2.25 2.4539 3.25 3.00 4.25 4.323 5.25 5.00 6.25 6.674 7.25 7.793 8.25 8.945 9.25 9.983}.

From Figs. 9–10, one may see that element location overlaps have been completely solved and the performance obtained was very acceptable.

4. Conclusions

The results obtained in the simulation have shown that non-uniformly spaced arrays with fully or partially absolute element location controls could offer a considerable improvement in terms of side lobe level reduction and also in terms of beamwidth. An equally narrow beamwidth as that of the standard uniformly spaced array was achieved by maintaining the same array aperture, i.e. by keeping the locations of the first and the last element constant. Consequently, similar directivity was obtained in the optimized array.

It was also observed that in non-uniformly spaced arrays, location overlaps were usually encountered between optimized elements – a phenomenon which is undesirable and may cause performance degradation in the practical applications of such arrays.

Two efficient approaches have been proposed to solve this problem. The first one relies on partially optimized element location controls, while the other one imposes bounded constraints on the location of each element. The principal advantage of using the two approaches proposed above is their short computational time. This feature is very important in the application of null placement for interference suppression. Thus, the proposed approaches can be extended to control the nulls in antenna array patterns by using randomly distributed elements with bounded constraints.

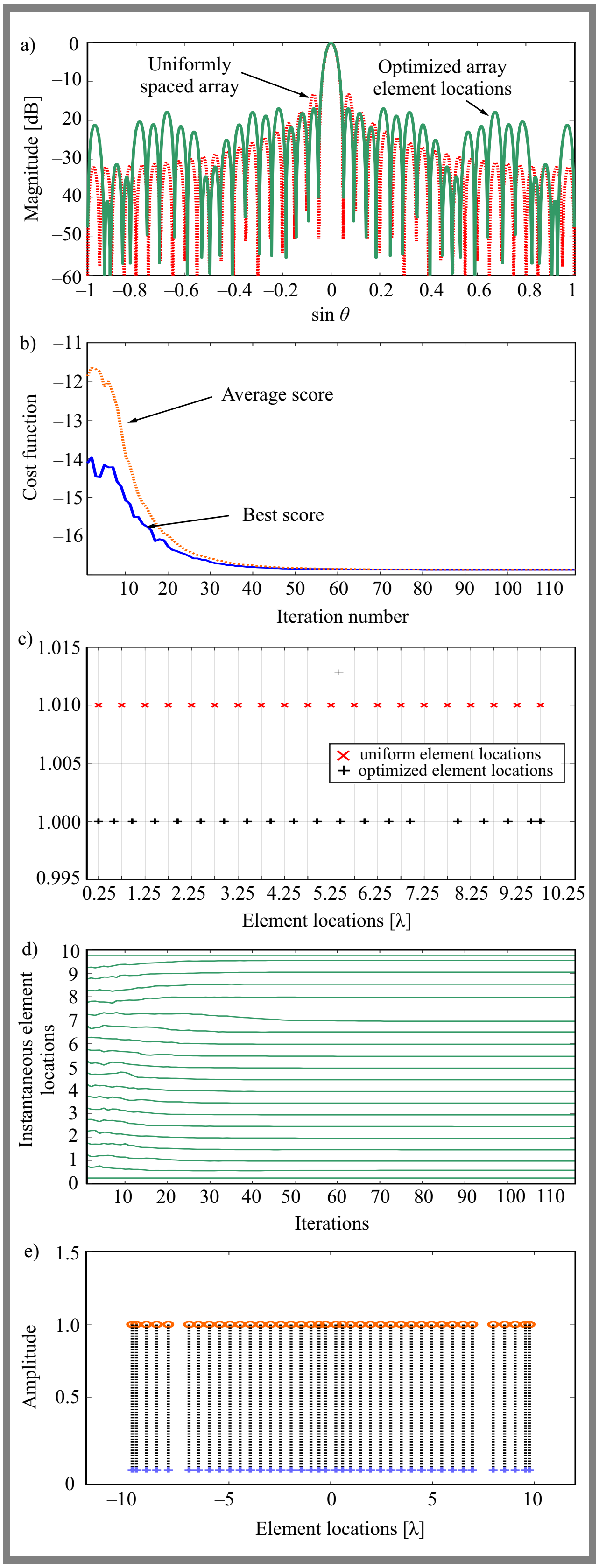

Fig. 9. Results of controlling all element locations with bounded constraints: a) radiation patterns, b) cost function variations, c) element locations, d) their instantaneous variations, and e) amplitude weights.

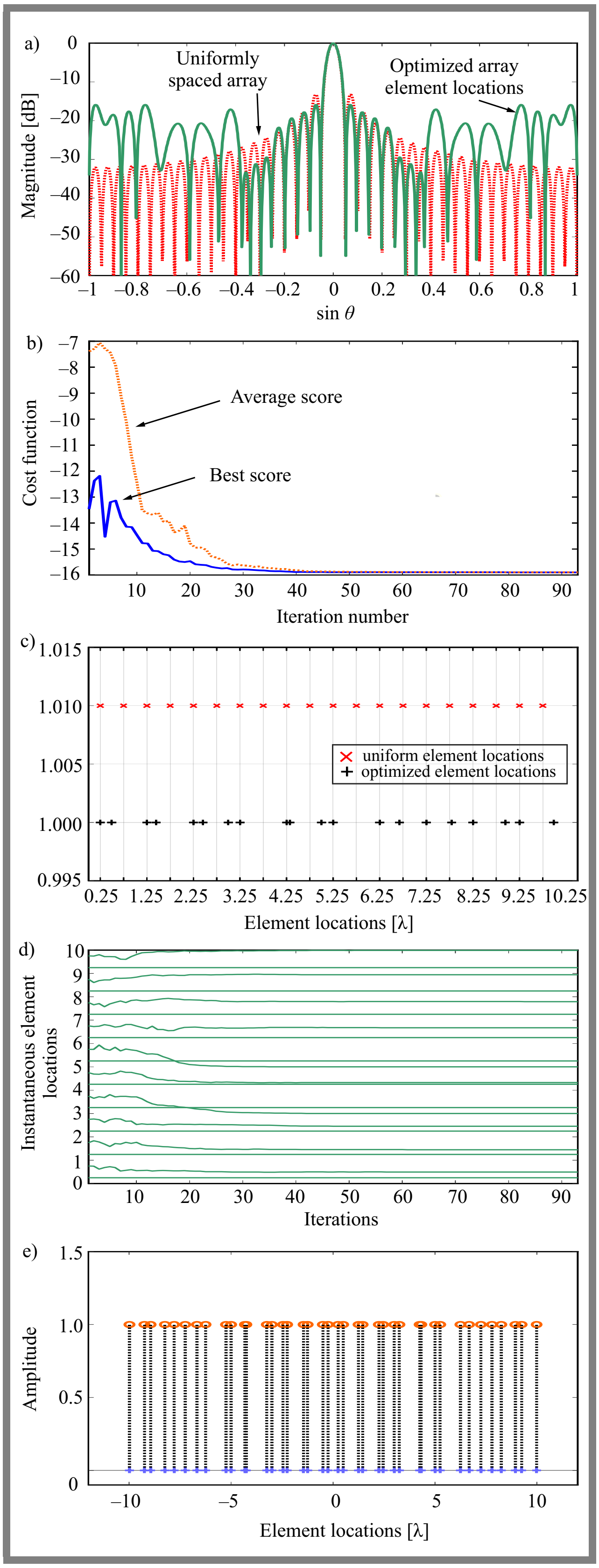

Fig. 10. Results of controlling half element locations with bounded constraints: a) radiation patterns, b) cost function variations, c) element locations, d) their instantaneous variations, and e) amplitude weights.

In contrast to sidelobe reduction, nulls placement requires a much lower number of the degrees of freedom, and these may be appropriately provided, in sufficient quantities, by the presented approaches. This should be the subject of future research work.

References

[1] A.J. Abdulqader, J.R. Mohammed, and R.H. Thaher, "Phase-only Nulling with Limited Number of Controllable Side Elements", *Progress in Electromagnetics Research C*, vol. 99, pp. 167–178, 2020 (https://doi.org/10.2528/PIERC20010203).

[2] J.R. Mohammed, A.J. Abdulqader, and R.H. Thaher, "Array Pattern Recovery under amplitude Excitation Errors Using Clustered Elements", *Progress in Electromagnetics Research M*, vol. 98, pp. 183–192, 2020 (https://doi.org/10.2528/PIERM20101906).

[3] J.R. Mohammed and K.H. Sayidmarie, "Sensitivity of the Adaptive Nulling to Random Errors in Amplitude and Phase Excitations in Array Elements", *Journal of Telecommunication, Electronic and Computer Engineering*, vol. 10, no. 1, pp. 51–56, 2018 (https://jtec.utem.edu.my/jtec/article/view/2023).

[4] M. Takuro and F. Mitoshi, "Reduction of Quantization Error Using Auxiliary Antenna on Array Antenna", *IEICE Communications Express*, vol.7, no.10, pp. 347–351, 2018 (https://doi.org/10.1587/comex.2018XBL0091).

[5] J.R. Mohammed and K.M. Younis, "Null Steering Implementation by Controlling Side-elements Positions", *International Journal of Microwave and Optical Technology*, vol. 16, no. 6, pp. 568–575, 2021.

[6] N. Anselmi, L. Tosi, P. Rocca, and A. Massa, "On the Design of Next Generation Phased Array Antennas - Methods, Architectures, and Trends", *2023 17th European Conference on Antennas and Propagation (EuCAP)*, Florence, Italy, 2023 (https://doi.org/10.23919/EuCAP57121.2023.10133211).

[7] J.R. Mohammed, "An Optimum Side Lobe Reduction Method with Weight Perturbation", *Journal of Computational Electronics*, vol.18, no. 2, pp. 705–711, 2019 (https://doi.org/10.1007/s10825-019-01323-5).

[8] J. Sanchez-Gomez, D.H. Covarrubias, and M.A. Panduro, "A Synthesis of Unequally Spaced Antenna Arrays Using Legendre Functions", *Progress In Electromagnetics Research M*, vol. 7, pp. 57–69, 2009 (https://doi.org/10.2528/PIERM09032305).

[9] J.R. Mohammed and K.H. Sayidmarie, "Synthesizing Asymmetric Side Lobe Pattern with Steered Nulling in Nonuniformly Excited Linear Arrays by Controlling Edge Elements", *International Journal of Antennas and Propagation*, vol. 2017, 2017 (https://doi.org/10.1155/2017/9293031).

[10] J.R. Mohammed, "Phased Array Antenna with Ultra-low Sidelobes", *Electronics Letters*, vol. 49, no. 17, pp. 1055—1056, 2013 (https://doi.org/10.1049/el.2013.1642).

[11] S.K. Goudos *et al.*, "Sparse Linear Array Synthesis with Multiple Constraints Using Differential Evolution with Strategy Adaptation", *IEEE Antennas and Wireless Propagation Letters*, vol. 10, pp. 670–673, 2011 (https://doi.org/10.1109/LAWP.2011.2161256).

[12] J.R. Mohammed, "Obtaining Wide Steered Nulls in Linear Array Patterns by Controlling the Locations of Two Edge Elements", *AEU International Journal of Electronics and Communications*, vol. 101, pp. 145–151, 2019 (https://doi.org/10.1016/j.aeue.2019.02.004).

[13] T.H. Ismail and M.M. Dawoud, "Null Steering in Phased Arrays by Controlling the Element Positions", *IEEE Transactions on Antennas and Propagation*, vol. 39, no. 11, pp. 1561–1566, 1991 (https://doi.org/10.1109/8.102769).

[14] A. Mukherjee, S.K. Mandal, and R. Ghatak, "Synthesis of Non-uniformly Spaced Planar Array Geometry Using Differential Evolution Algorithm", *2016 IEEE Indian Antenna Week (IAW 2016)*, Madurai, India, 2016 (https://doi.org/10.1109/IndianAW.2016.7883599).

[15] D.W. Boeringer and D.H. Werner, "Particle Swarm Optimization versus Genetic Algorithms for Phased Array Synthesis", *IEEE Transactions on Antennas and Propagation*, vol. 52, no. 3, pp. 771–779, 2004 (https://doi.org/10.1109/TAP.2004.825102).

[16] C. Zhang *et al.*, "Synthesis of Broadside Linear Aperiodic Arrays with Sidelobe Suppression and Null Steering Using Whale Optimization Algorithm", *IEEE Antennas and Wireless Propagation Letters*, vol. 17, no. 2, pp. 347–350, 2018 (https://doi.org/10.1109/LAWP.2018.2789919).

[17] G. Toso and P. Angeletti, "Optimal Combined Amplitude-density Synthesis of Aperiodic Arrays", *Proc. of the 5th European Conference on Antennas and Propagation (EUCAP)*, pp. 3044–3047, 2011 (https://ieeexplore.ieee.org/document/5782222).

[18] J.R. Mohammed, "Thinning a Subset of Selected Elements for Null Steering Using Binary Genetic Algorithm", *Progress in Electromagnetics Research M*, vol. 67, pp. 147–157, 2018 (https://doi.org/10.2528/PIERM18021604).

[19] A. Khan and J.S. Roy, "Design of Low Power Thinned Smart Antenna for 6G Sky Connection", *Journal of Telecommunications and Information Technology*, no. 1, pp. 26–33, 2024 (https://doi.org/10.26636/jtit.2024.1.1438).

[20] J.R. Mohammed, "A Method for Thinning Useless Elements in the Planar Antenna Arrays" *Progress In Electromagnetics Research Letters*, vol. 97, pp. 105–113, 2021 (https://doi.org/10.2528/PIERL21022104).

[21] A.J. Abdulqader, J.R. Mohammed, and Y.A. Ali, "A T-shaped Polyomino Subarray Design Method for Controlling Sidelobe Level", *Progress In Electromagnetics Research C*, vol. 126, pp. 243–251, 2022 (https://doi.org/10.2528/pierc22080803).

[22] J.R. Mohammed, "Simplified Rectangular Planar Array with Circular Boundary for Side Lobe Suppression", *Progress In Electromagnetics Research M*, vol. 97, pp. 57–68, 2020 (https://doi.org/10.2528/PIERM20062906).

[23] J. Hejres, "Null Steering in Phased Arrays by Controlling the Positions of Selected Elements", *IEEE Transactions on Antennas and Propagation*, vol. 52, no. 11, pp. 2891–2895, 2004 (https://doi.org/10.1109/TAP.2004.835128).

[24] L. Chen *et al.*, "Synthesis of Large-Scale Planar Isophoric Sparse Arrays Using Iterative Least Squares with Nonredundant Constraints (ILS-NRC)", *IEEE Transactions on Antennas and Propagation*, vol. 72, no. 5, pp. 4232–4245, 2024 (https://doi.org/10.1109/TAP.2024.3375971).

[25] P. You *et al.*, "Synthesis of Unequally Spaced Linear Antenna Arrays with Minimum Element Spacing Constraint by Alternating Convex Optimization", *IEEE Antennas and Wireless Propagation Letters*, vol. 16, pp. 3126–3130, 2017 (https://doi.org/10.1109/LAWP.2017.2764069).

Noor Mohammed Qassim, Student
College of Electronics Engineering
E-mail: noor.22enp29@student.uomosul.edu.iq
Ninevah University, Mosul, Iraq
https://uoninevah.edu.iq

Jafar Ramadhan Mohammed, Ph.D.
College of Electronics Engineering
https://orcid.org/0000-0002-8278-6013
E-mail: jafar.mohammed@uoninevah.edu.iq
Ninevah University, Mosul, Iraq
https://uoninevah.edu.iq